

Structure determination of L-arabinitol by powder X-ray diffraction

Patrick Derollez,* Yannick Guinet, Frédéric Affouard, Florence Danède, Laurent Carpentier and Alain Hédoux

Unité Matériaux et Transformations (UMR CNRS 8207), Université Lille 1, Sciences et Technologies, 59655 Villeneuve d'Ascq CEDEX, France

Correspondence e-mail:
patrick.derollez@univ-lille1.fr

Powder X-ray diffraction patterns of the commercial phase of L-arabinitol were recorded with a laboratory diffractometer. The starting structural model was found by a Monte-Carlo simulated annealing method. The final structure was obtained through Rietveld refinements with soft restraints on the interatomic bond lengths and bond angles. H atoms of hydroxyl groups were localized by minimization of the crystalline energy. The cell is triclinic with the space group *P1* and contains two molecules. The crystalline cohesion is achieved by an important network of O—H...O hydrogen bonds.

Received 5 January 2012

Accepted 3 May 2012

1. Introduction

Arabinitol, C₅H₁₂O₅, is a pentitol also called lyxitol or arabitol. It shows two enantiomorphs, D- and L-arabinitol. The D-arabinitol is naturally found in lichens and mushrooms. The L form is prepared by the catalytic reduction of arabinose. The crystallization of an aqueous solution of an equimolar mixture of the enantiomorphs gives racemic DL-arabinitol. The other two stereoisomeric pentitols are xylitol and ribitol. Xylitol is found in the fibers of fruits and vegetables. It is roughly as sweet as sucrose with lower food energy. Ribitol is formed by the reduction of ribose that occurs in certain plants and contributes to the structure of riboflavin. The crystal structures of xylitol and ribitol have been reported by Kim & Jeffrey (1969) and Kim *et al.* (1969). Until now, the structures of D- and L-arabinitol were not known. Only the crystal structure of racemic DL-arabinitol has been derived by X-ray diffraction on a single crystal (Hunter & Rosenstein, 1968). In this last compound the carbon chain conformation is planar, in contrast to the non-planar conformation in xylitol and ribitol. The cell of racemic arabinitol is orthorhombic and contains four molecules. The D and L enantiomers are related by glide planes in the space group *Pna2*₁. The molecule has a planar zigzag carbon chain with O atoms above and below the plane. All O atoms are involved in a hydrogen-bonding network formed by chains coiled around the screw axes.

It is well known that polyol materials are popular excipients in formulations for tableting, spray drying and freeze drying in pharmaceutical applications, and are also currently used in the food industry as glass-forming additives (Kadoya *et al.*, 2010). In this context, information on the physical properties (phase transformation temperatures, polymorphism, physical stability) should be relevant in the application of polyols to the manufacturing processes. Analysis of the crystalline conversion of amorphous states, and the complex polymorphic transitions of these materials (Nezzal *et al.*, 2009) are required to avoid unwanted crystallization. Understanding phase transformation mechanisms requires precise crystallographic

data on the different polymorphs of a variety of compounds belonging to the polyol family. Here we report the crystal structure determination of L-arabinitol prior to investigations of phase transformations in this compound.

The structure determination of the commercial L-arabinitol was performed at room temperature from powder X-ray diffraction experiments. The determination of the structure was solved *ab initio* using a direct-space approach (simulated annealing) and refined by Rietveld's method. Energy-minimization calculations were performed in order to locate the H-atom positions of the hydroxyl groups involved in hydrogen bonds.

2. Experimental

Commercial L-arabinitol (purity $\geq 98\%$) was purchased from Sigma-Aldrich Co. Samples were analysed without further purification. The X-ray powder diffraction patterns were measured on a laboratory diffractometer equipped with an INEL curved, position-sensitive detector (CPS120). The calibration of the detector was performed by the direct beam method. A bent quartz monochromator selected the $K\alpha_1$ wavelength of a Cu X-ray tube ($\lambda = 1.54056 \text{ \AA}$). The powder was introduced in a Lindemann glass capillary (diameter 0.7 mm) mounted on the axis of a G3000 goniometer. The sample was rotated during the measurements in order to reduce the effect of possible preferential orientations. Data were collected at room temperature in the 2θ range $0.2\text{--}95.8^\circ$ ($2\theta_{\text{step}} = 0.015^\circ$) with a total counting time of 22.5 h.

3. Structure solution

To determine the lattice parameters, the profile and the position of the 55 Bragg peaks with a 2θ angle lower than 47° were individually refined with the program *WinPlotr* (Roisnel & Rodriguez-Carvajal, 2002). Of these 30 ranging from 9 to 37° were introduced in the program *TREOR* (Werner *et al.*, 1985). All the reflections were indexed in a triclinic cell with the following lattice parameters: $a = 7.698$, $b = 9.720$, $c = 4.834 \text{ \AA}$, $\alpha = 96.1$, $\beta = 107.0$, $\gamma = 95.9^\circ$, $V = 340.5 \text{ \AA}^3$. The values of the figures of merit are: $M(30) = 26$, $F(30) = 55(0.017, 33)$ (de Wolff, 1968; Smith & Snyder, 1979). The *DICVOL* program (Boultif & Louër, 2004) also provides a unique solution close to the previous cell: $a = 7.674$, $b = 9.707$, $c = 4.824 \text{ \AA}$, $\alpha = 96.1$, $\beta = 106.8$, $\gamma = 96.0^\circ$, $V = 338.6 \text{ \AA}^3$ with the following values of the figures of merit: $M(30) = 46$, $F(30) = 105(0.007, 43)$. The volume of the cell is approximately half those of DL-arabinitol (Hunter & Rosenstein, 1968). Therefore, the number of molecules in the cell (Z) is 2. Among the two possible triclinic space groups, $P\bar{1}$ is forbidden because the inversion centre leads to the presence of both enantiomers in the sample. Thus, the only possible space group is $P1$ with a cell containing two independent molecules.

In order to confirm the cell parameters found, refinements were carried out with the 'profile-matching' option (Le Bail *et al.*, 1988) of the program *FullProf* (Rodriguez-Carvajal, 2001). The angular range used for these refinements was from 5 to

Table 1

Crystallographic data, profile and structural parameters for L-arabinitol obtained after Rietveld refinements.

Crystal data	
Chemical formula	$C_5H_7(OH)_5$
M_r	152.15
Crystal system, space group	Triclinic, $P1$
a, b, c (Å)	7.6798 (2), 9.7170 (3), 4.8286 (1)
α, β, γ (°)	96.039 (1), 106.806 (1), 96.094 (1)
V (Å ³)	339.48 (2)
Z	2
Radiation type	$\lambda = 1.54056 \text{ \AA}$
μ (mm ⁻¹)	1.17
Specimen shape, size (mm)	Cylinder, 0.7
2θ range (°)	5.0–95.8
Data collection	
Diffractometer	Inel CPS120
Specimen mounting	0.7 mm diameter Lindemann capillary
Data collection mode	Transmission
Scan method	Stationary detector
Step size (° 2θ)	0.015
2θ values (°)	$2\theta_{\text{fixed}} = 0.2\text{--}95.8$
Refinement	
R -factors and goodness-of-fit (corrected for background)	$R_p = 0.073$, $R_{wp} = 0.078$, $R_{exp} = 0.024$, $R_{Bragg} = 0.032$, $\chi^2 = 10.7$
R -factors and goodness-of-fit (not corrected for background)	$R_p = 0.029$, $R_{wp} = 0.039$, $R_{exp} = 0.012$, $R_{Bragg} = 0.032$, $\chi^2 = 10.7$
No. of profile data steps	6379
No. of contributing reflections	638
No. of structural, profile parameters	60, 13
No. of background points refined	24
No. of bond length, bond angle constraints	18, 22
U, V, W	0.134 (7), -0.065 (4), 0.033 (1)
η_0	0.654 (6)
Asym ₁ , Asym ₂	0.0729 (22), -0.0077 (4)
B_{iso} carbon, oxygen atoms (Å ²)	1.38 (6), 2.03 (5)

$96^\circ 2\theta$. The profile of the Bragg peaks was fitted with a pseudo-Voigt function with the same FWHM for the Gaussian and the Lorentzian components. This FWHM has a θ dependence according to the Caglioti function (Caglioti *et al.*, 1958). The asymmetry of the Bragg peaks was taken into account according to the Bélar and Baldinozzi function (Bélar & Baldinozzi, 1993). The background was determined with a linear interpolation between 24 points regularly distributed from 5 to 96° . The 37 refined parameters are as follows: the lattice parameters a, b, c, α, β and γ , the zero-shift, the Caglioti profile parameters U, V, W , the mixing parameter of the pseudo-Voigt function η_0 , 2 parameters for the asymmetry of the Bragg peaks and 24 points to define the background. At the end of the 'profile matching' refinements, the profile reliability factors (corrected for background) are: $R_p = 0.051$, $R_{wp} = 0.055$, $R_{exp} = 0.024$ and $\chi^2 = 5.4$; the lattice parameters are $a = 7.6785$ (1), $b = 9.7142$ (2), $c = 4.8271$ (1) Å, $\alpha = 96.035$ (1), $\beta = 106.806$ (1), $\gamma = 96.090$ (1) $^\circ$ and $V = 339.23$ (1) Å³. An NAC (Na₂Ca₃Al₂F₁₄; Evain *et al.*, 1993) standard compound was used to obtain the experimental resolution. The comparison of the widths of both compounds show no microstructural effects (size of crystallites and micro-strain effects).

Table 2
Values of the bond lengths (Å) and angles (°) for L-arabinitol.

	Molecule <i>a</i>	Molecule <i>b</i>
C1—C2	1.521 (2)	1.527 (6)
C2—C3	1.523 (4)	1.516 (3)
C3—C4	1.519 (3)	1.513 (4)
C4—C5	1.523 (7)	1.517 (4)
C1—O1	1.438 (6)	1.437 (8)
C2—O2	1.437 (8)	1.437 (7)
C3—O3	1.431 (6)	1.427 (7)
C4—O4	1.440 (7)	1.440 (7)
C5—O5	1.441 (9)	1.436(7)
C2—C1—O1	113.0 (4)	106.7 (6)
C1—C2—C3	111.8 (2)	118.7 (4)
C1—C2—O2	107.6 (5)	106.7 (7)
C3—C2—O2	111.7 (6)	113.1 (5)
C2—C3—C4	114.3 (3)	117.7 (3)
C2—C3—O3	111.0 (5)	104.3 (5)
C4—C3—O3	103.9 (4)	109.5 (7)
C3—C4—C5	118.1 (4)	115.3 (4)
C3—C4—O4	105.7 (5)	103.4 (6)
C5—C4—O4	110.5 (7)	111.8 (5)
C4—C5—O5	112.0 (7)	109.5 (5)

In order to obtain a starting structural model, the ‘parallel tempering’ algorithm of the program *FOX* (Favre-Nicolin & Černý, 2002) was used. The molecule of L-arabinitol is built with bond lengths, bond angles and torsion angles calculated from the atomic coordinates of Hunter & Rosenstein (1968) obtained from the structure determination of DL-arabinitol. This molecule is introduced randomly in the cell. The relaxed restraints option used for the calculations modifies the bond lengths, bond angles and torsion angles. Atomic coordinates found by *FOX* were introduced in the program *FullProf* (Rodríguez-Carvajal, 2001) in order to perform Rietveld refinements. Soft restraints on the bond lengths and bond angles were applied. Standard deviations for restraint values

in the final calculations were equal to 0.003 Å for bond lengths and 0.5° for bond angles.

Some H atoms can be placed with geometrical arguments. For example, this is the case for the CH and CH₂ groups. Each C atom is at the centre of a tetrahedron and the H atoms complete these tetrahedra with a bond length C—H equal to 1.00 Å. The positions of the H atoms of the OH groups involved in hydrogen bonds were determined using the energy minimization of L-arabinitol. Similar calculations have been applied successfully in the structural determination of a 1/1 α/β mixed lactose (Lefebvre *et al.*, 2005) and the stable anhydrous phase of α -lactose (Platteau *et al.*, 2005). Computations were performed using the *DLPOLY* program (Smith & Forester, 1996) using the all-atom general amber force field (GAFF; Wang *et al.*, 2004) to model the intra- and intermolecular interactions. The initial configuration of the system was constructed from $N = 250$ L-arabinitol molecules ($5 \times 5 \times 5$ crystalline cells with $Z = 2$). A cutoff radius of 10 Å was used to account for van der Waals interactions. A Lennard–Jones potential was employed to represent van der Waals interactions and Lorentz–Berthelot mixing rules were used for cross-interaction terms. Atomic charges were derived from the AM1-b.c.c. method using the program *ANTECHAMBER* (Wang *et al.*, 2004). Electrostatic interactions were handled by an Ewald summation method. Energy minimization calculations were carried out from the structure obtained experimentally. In order to maintain L-arabinitol structure as close as possible to the structure determined from X-ray diffraction, the positions of all atoms were not allowed to move, except the positions of the H atoms of the hydroxyl groups. If the whole structure is minimized, a change of less than 5% of the cell parameters and atomic positions with respect to the experimental values is observed. This distortion is reasonable for the GAFF force-field used in the present calculation since this force-field is not optimized for crystal

structure prediction. The overall hydrogen-bond network is preserved. Moreover, it should be mentioned that the stability of the proposed L-arabinitol structure was also successfully confirmed using molecular dynamics (MD) simulations performed at different temperatures using the *DLPOLY* program (Smith & Forester, 1996). In these MD simulations, no constraints on the atomic positions were imposed.

Therefore, for the Rietveld refinements, there are 97 adjustable parameters:

37 lattice parameter, background and line-shape parameters as described above.

60 structural parameters: the scale factor, two isotropic displacement parameters for C and O

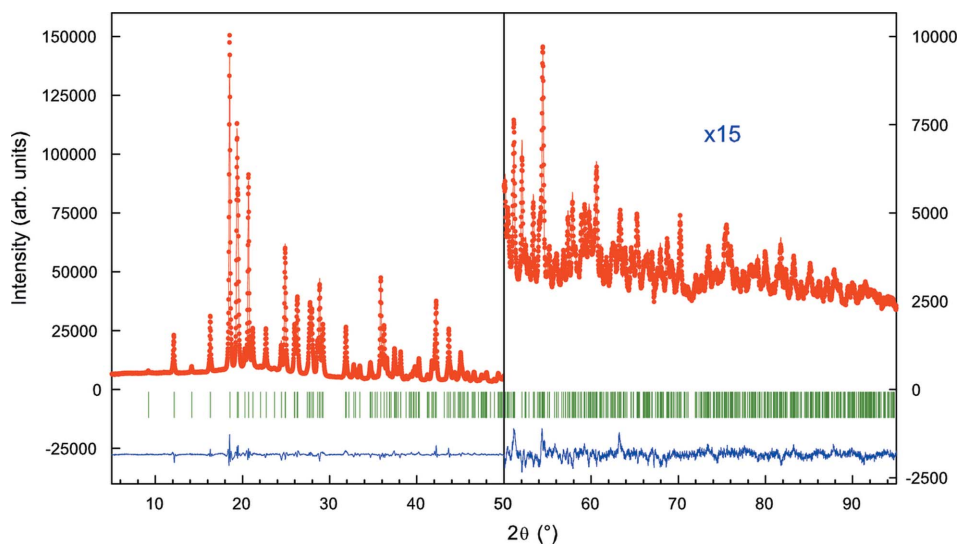


Figure 1

Final Rietveld plot of the L-arabinitol. Observed data points are indicated by dots, the best-fit profile (upper trace) and the difference pattern (lower trace) are shown as solid lines. The vertical bars correspond to the positions of the Bragg peaks.

Table 3

Least squares planes in L-arabinitol.

The equation used is $AX + BY + CZ = D$, where X, Y, Z are in Å.

		Deviation in Å from plane		Fitted parameters of the plane	
Molecule <i>a</i>	C1	-0.028			
	C2	-0.021	<i>A</i>	-1.378	
	C3	0.074	<i>B</i>	2.333	
	C4	0.023	<i>C</i>	-0.227	
	C5	-0.049	<i>D</i>	0.725	
Molecule 2	C1	0.003			
	C2	-0.086	<i>A</i>	-1.177	
	C3	0.084	<i>B</i>	2.308	
	C4	0.080	<i>C</i>	0.008	
	C5	0.081	<i>D</i>	13.952	

Table 4

Hydrogen-bonding geometry (Å, °) for the L-arabinitol.

<i>D</i> —H··· <i>A</i>	<i>D</i> —H	H··· <i>A</i>	<i>D</i> ··· <i>A</i>	<i>D</i> —H··· <i>A</i>
O1 <i>a</i> —HO1 <i>a</i> ···O4 <i>b</i> ⁱ	0.85	2.07	2.90	165.9
O2 <i>a</i> —HO2 <i>a</i> ···O5 <i>a</i> ⁱⁱ	1.03	1.69	2.72	173.0
O3 <i>a</i> —HO3 <i>a</i> ···O2 <i>a</i> ⁱⁱⁱ	1.01	1.69	2.71	176.1
O4 <i>a</i> —HO4 <i>a</i> ···O1 <i>b</i> ⁱ	0.95	1.87	2.82	177.2
O5 <i>a</i> —HO5 <i>a</i> ···O4 <i>a</i> ⁱⁱⁱ	1.04	1.70	2.74	170.6
O1 <i>b</i> —HO1 <i>b</i> ···O1 <i>a</i> ^{iv}	0.98	1.75	2.73	176.2
O2 <i>b</i> —HO2 <i>b</i> ···O3 <i>b</i> ^v	1.05	1.72	2.77	174.8
O3 <i>b</i> —HO3 <i>b</i> ···O3 <i>a</i> ^{vi}	0.92	1.90	2.82	175.2
O4 <i>b</i> —HO4 <i>b</i> ···O5 <i>b</i> ^v	0.99	1.75	2.73	175.4
O5 <i>b</i> —HO5 <i>b</i> ···O2 <i>b</i> ^{vii}	0.97	1.79	2.77	177.8

Symmetry codes: (i) $x, y - 1, z$; (ii) $x - 1, y, z$; (iii) $x, y, z - 1$; (iv) $x + 1, y + 1, z$; (v) $x, y, z + 1$; (vi) x, y, z ; (vii) $x - 1, y, z - 1$.

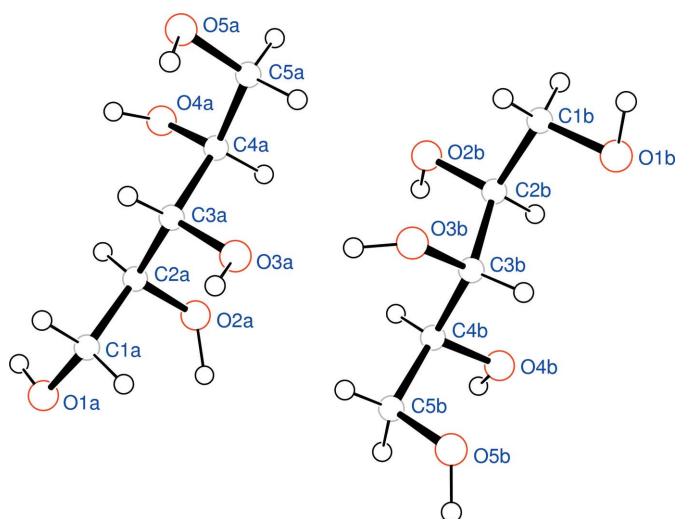


Figure 2

Atomic numbering and structure of the molecules of L-arabinitol.

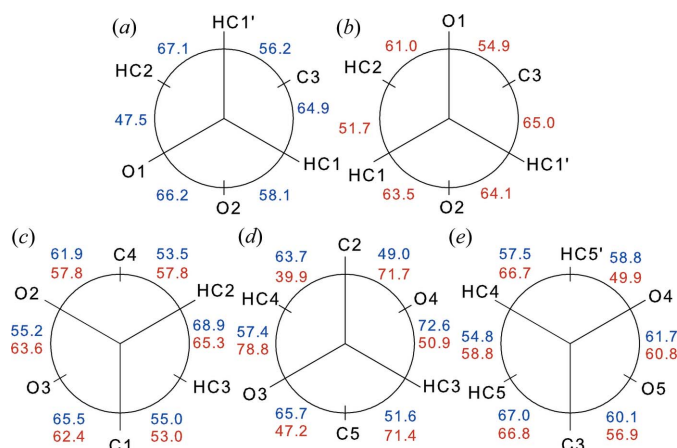


Figure 3

Conformation angles (°) for the L-arabinitol. The Newman projections are of: the C1—C2 bond: (a) molecule *a* and (b) molecule *b*; the C2—C3, C3—C4, C4—C5 bonds: (c), (d) and (e) respectively. The upper values concern the angles of molecule *a* and the lower values the angles of molecule *b*.

atoms, and 57 atomic coordinates of the non-H atoms. The position of the C1*a* atom is fixed and defines the origin of the cell. No preferred orientations of the sample in the capillary could be showed in the Bragg peak refinements.

The final conventional (corrected for background) Rietveld agreement factors are: $R_p = 0.073$, $R_{wp} = 0.078$, $R_{exp} = 0.024$ and $\chi^2 = 10.7$. The mean-square deviations from the soft restraints are 0.005 Å for the bond lengths and 3.5° for the bond angles. The mean value of the electronic density synthesis is zero with a mean-square deviation of 0.01 e Å⁻³, the values of the highest peak and the deepest hole being equal to 0.03 and -0.04 e Å⁻³. The experimental and calculated diffraction patterns are shown in Fig. 1. A representation of the molecule drawn with ORTEP3 (Farrugia, 1997) and the numbering of the atoms is shown in Fig. 2. Crystallographic data, profile and structural parameters are given in Table 1 and values of the bond lengths and bond angles are given in Table 2.¹

4. Discussion

The mean values of the C—C bond lengths are 1.521 (2) and 1.518 (5) Å in molecules *a* and *b*, respectively. The mean values of the C—O bond lengths are 1.437 (3) and 1.435 (4) Å. For the valence angles, the mean values are 114.7 (2.6) and 117.2 (1.4)° for the C—C—C angles, 109.4 (3.1) and 108.1 (3.2)° for the C—C—O angles in molecules *a* and *b*, respectively. For each type of molecule, the carbon skeleton is planar as observed in racemic DL-arabinitol but not in xylitol and ribitol. The out-of plane distance of the C atoms is lower than 0.08 Å for molecule *a* and 0.09 Å for molecule *b* (see Table 3). The values of the dihedral angles are shown in Fig. 3. The conformation angles around the C2—C3 and C4—C5 bonds (Figs. 3c–e) are close for both types of molecules. Differences occur on conformation angles around the C3—C4 bond (Fig. 3d) with a shift higher than 20°. The major difference is observed on the terminal hydroxyl group connected to

¹ Supplementary data for this paper are available from the IUCr electronic archives (Reference: PS5016). Services for accessing these data are described at the back of the journal.

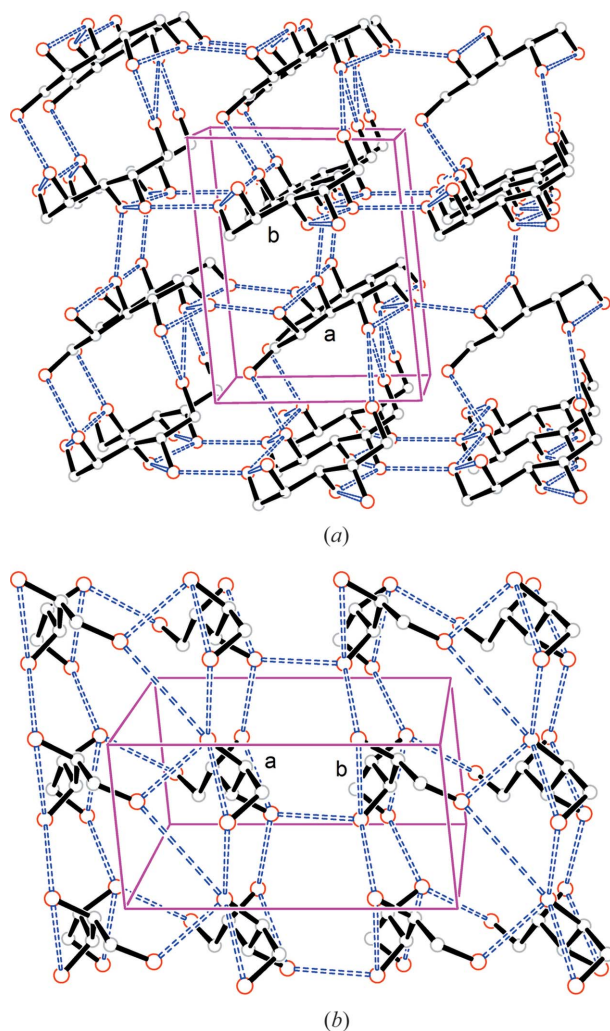


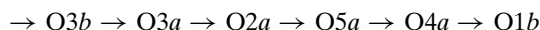
Figure 4
(a) Perspective drawing normal to the (001) plane of L-arabinitol (horizontal axis **a**) and (b) normal to the (100) plane (horizontal axis **b**).

the C1 atom which differs by a rotation of about 120° from one type of molecule to another (Figs. 3a and b).

The molecules lie in planes connected by a network of hydrogen bonds, as depicted in Fig. 4. Within the planes, molecules *a* and *b* alternate along the direction of chains, formed by $O1b-HO1b \cdots O1a^{iv}$ hydrogen bonds (the symmetry code is given in Table 4). Two molecules of type *a* are joined in the **a** direction by a $O2a-HO2a \cdots O5a^{ii}$ hydrogen bond. In the **b** direction, a molecule *a* is connected with a molecule *b* via the $O3b-HO3b \cdots O3a^{vi}$ bond. Finally, in the **c** direction, molecules of type *a* are joined with the $O3a-HO3a \cdots O2a^{iii}$ and $O5a-HO5a \cdots O4a^{iii}$ hydrogen bonds and molecules of type *b* with the $O2b-HO2b \cdots O3b^v$

and $O4b-HO4b \cdots O5b^v$ bonds. Characteristics of the hydrogen bonds are reported in Table 4, employing the hypothesis that, for a hydroxyl group, an O atom can be a donor only once, but it can be an acceptor several times.

The $O \cdots O$ distances range from 2.71 to 2.90 Å with an average value of 2.77 Å with a root mean-square deviation of 0.06 Å. In racemic DL-arabinitol, the average value is 2.73 Å (Hunter & Rosenstein, 1968). We observe that all hydroxyl groups are involved in hydrogen bonds; each of them forms one donor and one acceptor bond. The hydrogen bond network forms infinite chains having the donor sequence



Such a sequence of infinite chains is also observed in racemic arabinitol.

References

- Bérar, J.-F. & Baldinozzi, G. (1993). *J. Appl. Cryst.* **26**, 128–129.
 Boultif, A. & Louër, D. (2004). *J. Appl. Cryst.* **37**, 724–731.
 Caglioti, G., Paoletti, A. & Ricci, F. P. (1958). *Nucl. Instrum.* **3**, 223–228.
 Evain, M., Deniard, P., Jouanneaux, A. & Brec, R. (1993). *J. Appl. Cryst.* **26**, 563–569.
 Farrugia, L. J. (1997). *J. Appl. Cryst.* **30**, 565.
 Favre-Nicolin, V. & Cerný, R. (2002). *J. Appl. Cryst.* **35**, 734–743.
 Hunter, F. D. & Rosenstein, R. D. (1968). *Acta Cryst.* **B24**, 1652–1660.
 Kadoya, S., Fujii, K., Izutsu, K., Yonemochi, E., Terada, K., Yomota, C. & Kawanishi, T. (2010). *Int. J. Pharm.* **389**, 107–113.
 Kim, H. S. & Jeffrey, G. A. (1969). *Acta Cryst.* **B25**, 2607–2613.
 Kim, H. S., Jeffrey, G. A. & Rosenstein, R. D. (1969). *Acta Cryst.* **B25**, 2223–2230.
 Le Bail, A., Duroy, H. & Fourquet, J. L. (1988). *Mater. Res. Bull.* **23**, 447–452.
 Lefebvre, J., Willart, J.-F., Caron, V., Lefort, R., Affouard, F. & Danède, F. (2005). *Acta Cryst.* **B61**, 455–463.
 Nezzal, A., Aerts, L., Verspaille, M., Henderickx, G. & Redl, A. (2009). *J. Cryst. Growth*, **311**, 3863–3870.
 Platteau, C., Lefebvre, J., Affouard, F., Willart, J.-F., Derollez, P. & Mallet, F. (2005). *Acta Cryst.* **B61**, 185–191.
 Rodriguez-Carvajal, J. (2001). *FullProf*, Version 1.9c. LLB, CEA/Saclay, France.
 Roisnel, T. & Rodriguez-Carvajal, J. (2002). *Mater. Sci. Forum*, **378–381**, 118–123.
 Smith, W. & Forester, T. R. (1996). *J. Mol. Graph.* **14**, 136–141.
 Smith, G. S. & Snyder, R. L. (1979). *J. Appl. Cryst.* **12**, 60–65.
 Wang, J., Wolf, R. M., Caldwell, J. W., Kollman, P. A. & Case, D. A. (2004). *J. Comput. Chem.* **25**, 1157–1174.
 Werner, P.-E., Eriksson, L. & Westdahl, M. (1985). *J. Appl. Cryst.* **18**, 367–370.
 Wolff, P. M. de (1968). *J. Appl. Cryst.* **1**, 108–113.